Random walk and directed movement: comparison between inert particles and self-organized molecular machines

M. Schienbein, K. Franke, and H. Gruler
Abteilung Biophysik, Universität Ulm, D89069 Ulm, Germany
(Received 19 November 1993)

The differences and similarities between the behavior of inert particles exposed to force fields and of biological cells exposed to guiding fields are shown. Cell migration can be characterized by two independent variables: the speed v which is controlled by a steering device and the migration angle φ which is controlled by an automatic pilot. Each variable is described by a stochastic differential equation. The cellular behavior can be obtained by solving the corresponding Fokker-Planck equations. The predicted dose-response curve (the dose is the guiding field as electric field or concentration gradient, the response is the polar order parameter) fits quite well the experimental data obtained for different cell types. The predicted field dependence of the first eigenvalue is in accordance with the measured ones. The limitation of the model is discussed.

PACS number(s): 82.70.−y, 87.10.+e, 87.22.Nf

INTRODUCTION

Many natural scientists are fascinated by the ability of single cells of the immune system to detect, respond to, and destroy microorganisms. Embryogenesis and wound healing are other examples, to name two, where directed and nondirected cell movement is involved [1–3]. The purpose of the present work is to study the basic differences between directed cell movement induced by an extracellular guiding field, and directed movement of an inert particle induced by an external force.

Our investigations are basically performed with human granulocytes which form the first defense line against invading microorganisms. These cells migrate like an amoeba by changing their shape. The basic biochemical reactions of the cellular signal transduction chain are known [4]. But the physical events are less understood.

First we want to summarize what is known about the cellular signal transduction chain of granulocytes. One main function of the membrane is to separate the intracellular space from the extracellular space. In addition to this main function, the membrane also is the first element in the signal transduction chain. *Step 1:* Intracellular calcium forces vesicles (loaded with fresh receptors) to fuse with the plasma membrane. *Step 2:* Specific molecules stimulating chemokinesis and chemotaxis bind to the new exposed receptors. *Step 3:* The activated receptors are the first elements in the biochemical amplification chain. One loaded receptor activates many membrane-attached G proteins. One G protein activates many phospholipase-C molecules. One phospholipase-C molecule hydrolyzes many ATP-activated phospholipid (phosphatidylinositol) molecules at the inner side of the membrane. *Step 4:* The head group inositol triphosphate opens calcium channels and internal calcium stores and the remaining lipid diacylglycerol destabilizes the plasma membrane locally. *Step 5:* The increased intracellular calcium concentration triggers several cellular functions. First, the amoeboid migration of the cell is induced by the calcium triggered adhesion of the plasma membrane to a substrate and by the calcium dependent activation of micofilaments (muscles) [5,6]. Second, vesicles loaded with fresh receptors are forced to fuse with the plasma membrane. This fusion process is induced by the increased local calcium concentration and by the locally destabilized plasma membrane. With the vesicle fusion a new cycle starts (self-ignition model [7]).

One would like to investigate the isolated motile apparatus of a cell as a model of self-organized molecular machines. Keller and Bessis [8] had come upon just such a self-purification of the motile machinery some time ago in granulocytes subjected to the carefully controlled and timed application of heat. This treatment causes the leading edge (motor) of the cell to move forward rapidly, forming a long thin stalk of cytoplasm that often breaks to form two separate units, the cytokineplast (fragments) and the cell body. The machinery which creates the cell locomotion contains only a few elements: a part of the plasma membrane, unstructured cytoplasm as seen by light microscopy, and the necessary biochemistry. Most important, the newly formed fragments were capable of membrane movement, including adherence, spreading, random locomotion, directed movement, and phagocytosis [9,10].

The directed movement like chemotaxis, galvanotaxis, etc., are functions of cells having a goal-seeking system. Due to the noise in the system, these functions are described by stochastic differential equations [11–13]. Thus directed cell movement is described in the framework of the Smoluchowski equation [14], which is known to describe the Brownian motion of a particle in a potential.

Macroscopic physical systems are subject to fluctuations or noise. To name a few examples:

(1) Irregular movement of small colloidal particles, caused by the impacts of the molecules of the liquid, was described by Brown [15], Pearson [16], Lord Rayleigh [17], Einstein [18], v. Smoluchowski [19], Fürth [20], Langevin [21] and others [22].

(2) Schottky [23,24] described the fluctuations in

emission-limited current flow in thermionic diodes carried by single and independent emitted electrons. Nyquist [25] investigated the thermal equilibrium noise arising in an electrical transmission line terminated by a resistor.

(3) The effect of noise in nonlinear circuits was reviewed by Lax [26]. Many systems of engineering interest are nonlinear.

(4) The development of the laser acted as a further spur to the study of noise. There, fluctuations are considered in systems which are not in thermal equilibrium. Haken [27] reviewed stochastic phenomena in systems far from equilibrium.

(5) The effect of noise in self-organized entities which are far from thermal equilibrium is discussed in the present paper. Only the phenomenon of the directed cell movement will be discussed here. The physical aspects of the molecular events will be discussed somewhere else.

The modern analysis of noise was introduced by Kramers [28]. The population dynamics of a locally stable state is determined by the transition kinetics between competing states. For example, he treated the escape from a potential well as a problem of Brownian motion in a nonuniform force field (see [29]).

An important concept in understanding biological phenomena is the theory of automatic control [30]. It is shown [11–13] that chemotaxis, galvanotaxis, etc. are functions of cells having a goal-seeking system. Even when the involved physicochemical signals are unknown, the cellular system can be considered phenomenologically as an automatic controller having a closed-loop feedback system.

The cellular signal transduction-response system can be approximated by two types of signals [11,12,14], a deterministic and a stochastic one. If the automatic controller acted deterministically then in galvanotaxis, for example, the cells would exactly follow the (straight) electric-field lines. However, the observed trajectories are snakelike curves toward the desired direction. Next, the cell migration is compared with the motion of an inert particle.

BROWNIAN MOTION, RANDOM WALK, AND LANGEVIN EQUATION

In the studies on Brownian motion of inert particles, one is principally concerned with the perpetual irregular motion exhibited by small grains or particles of colloidal size immersed in a fluid. The perpetual motion of the Brownian particles is maintained by the collisions with the molecules of the surrounding fluid. Under normal conditions, in a liquid, a Brownian particle will suffer about 10^{11} collisions per second and this is so frequent that one cannot speak of separate collisions. The result is a time-dependent force $\mathbf{F}(t)$, which describes the interaction of the inert particle with the surrounding liquid molecules. It is obvious that the average of $\mathbf{F}(t)$ is zero. This time-dependent force per mass, $\mathbf{F}(t) = -\gamma\mathbf{v} + \mathbf{\Gamma}(t)$, can be separated into two parts. (i) $-\gamma\mathbf{v}$ describes the damping of the slow motion by friction (γ is the friction coefficient) and (ii) the stochastic term, $\mathbf{\Gamma}(t)$ describes the fast motion of the inert particle. The Langevin equation for Brownian motion is then [31]

$$\frac{d\mathbf{v}}{dt} = -\gamma\mathbf{v} + [\mathbf{F}_{\text{ext}}(\mathbf{r},t)] + \mathbf{\Gamma}(t) \tag{1}$$

where $\mathbf{v}$ denotes the velocity of the particle. For the fluctuating part, $\mathbf{\Gamma}(t)$, the following principal assumptions are made.

(i) $\mathbf{\Gamma}(t)$ is independent of $\mathbf{v}$.

(ii) $\mathbf{\Gamma}(t)$ varies extremely rapid compared to the variations of $\mathbf{v}$.

In the presence of an external field or force, the Langevin equation (Eq. 1) is enlarged by $\mathbf{F}_{\text{ext}}(\mathbf{r},t)$, the external force divided by the mass m.

In contrast to inert particles, living cells are self-organized molecular entities which have the ability to migrate actively. Cells like granulocytes (Fig. 1), fibroblasts, neural crest cells, etc., migrate in an amoeboid way on a substrate and have the ability to respond to extracellular chemical and physical signals resulting in directed and nondirected movement. In *chemokinesis*, the chemical environment of the cells stimulates the migration, which is quantified by the mean speed. If the chemical environment of the cell is spatially dependent, then the cellular migration is guided in such a way that the cells drift on average parallel to the concentration gradient. This type of movement is quantified by the mean drift velocity and referred to as *chemotaxis*. If an electric field is used as guiding field, the cellular migration is referred to as *galvanotaxis*. Typical trajectories of a migrating granulocyte exposed to an electric field are shown in Fig. 2. A detailed description of the self-organized molecular machine will be given somewhere else [7]. Here we will concentrate our attention on the phenomenological properties of the cellular automatic pilot.

The translational movement in a polar guiding field

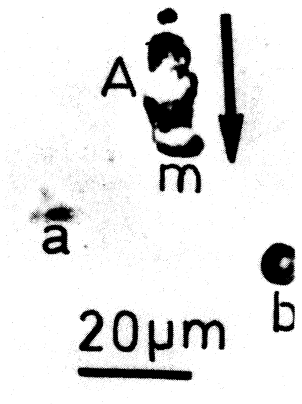

FIG. 1. Micrograph (phase contrast) of different blood cells in a sandwich cell [glass slide, aqueous solution (blood plasma, $d \approx 20\,\mu$m) coverslip]. (i) Human granulocyte (A) [leading front (m) and direction of migration (arrow)], (ii) platelet (a), and (iii) erythrocyte (b).

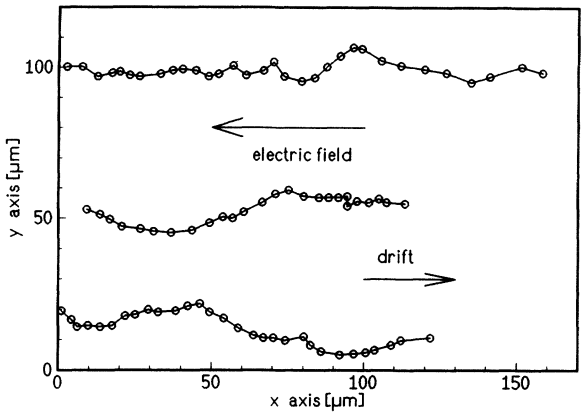

FIG. 2. Typical trajectories of granulocytes exposed to an electric field ($E = 0.8$ V/mm, time increment $\Delta t = 10$ s).

like an electric field requires two components of the cellular response (movement in two dimensional space), the speed v and the migration direction φ. One might well expect that these two parameters depend on each other, but actually they are independent. Experimental facts are that (i) the temporal fluctuations of v(t) and φ(t) are independent of each other, (ii) the mean speed is independent of the migration angle, and (iii) in galvanotaxis, for example, the mean speed is independent of the electric guiding field strength. This holds true at least for human granulocytes and monocytes [32–34], somitic fibroblasts [35,36], and neural crest cells [37]. Thus, the speed and the migration angle can be regarded as two independent variables. Each variable can be described by a stochastic differential equation, a Langevin equation [12,14]. In fact, the migrating cells can be compared with a driven car where the amount of speed, adjusted by the gas pedal, and the direction of motion, adjusted by the steering wheel, can be independently altered.

Thus, the basic difference between the motion of an inert particle and that of a migrating cell is as follows. The speed of an inert particle is given by the thermal energy. The velocity component in the direction of an applied force increases if an external force acts on the inert particle. The mean speed of a migrating cell is simply given by the cellular motor which is activated by molecules (chemokinetic stimuli) of the extracellular space. The mean cellular speed is proportional to the number of receptors loaded with chemokinesis stimulating molecules.

Langevin equation for the speed

A single cell alters its speed in a nonpredictable fashion. Thus, stochastic processes are involved in the cellular signal transduction-response system. The simplest nontrivial stochastic differential equation is assumed for the speed [12,14],

$$\frac{dv}{dt} = -\gamma_v\, v + \gamma_v\, v_s + \Gamma_v(t). \tag{2}$$

Let us assume that only the first term on the right side is nonzero. Then the remaining deterministic differential equation describes an exponential decay of the speed as a function of time. The characteristic time of the exponential decay function is given by γ_v^{-1}. Now, let us assume the first and the second terms on the right side are nonzero. Then the exponential decay of the velocity approaches a finite speed v_s. The cellular signal transduction-response system has a constant chemical amplification since the mean speed is proportional to the total number of membrane-bound receptors loaded with chemokinesis stimulating molecules [11,13,38–40]. The third term Γ_v(t) on the right side of the equation characterizes the stochastic process involved in the signal transduction-response system of the cell. The stochastic nature of $\Gamma(t)_v$ is not caused by the collisions with the molecules of the surrounding fluid but is a property of the physicochemical processes involved in the cellular signal transduction-response system.

Langevin equation for the migration angle

One important biological function of cells is their capacity for directed movement. The simplest nontrivial stochastic differential equation for the migration angle is

$$\frac{d\varphi}{dt} = -c_1 \sin\varphi + \Gamma_\varphi(t). \tag{3}$$

The first term on the right side of this equation describes the deterministic torque where $\sin\varphi$ is the first nontrival term of a Fourier series which is in accordance with the symmetry of the system. The physical state is unchanged if the coordinate system is rotated by 2π and in the absence of chirality the torque changes sign if the coordinate system is inverted at the line defined by the polar guiding field. In the small angle approximation ($\sin\varphi \approx \varphi$) this term can be interpreted as the torque induced by a proportional controller ($d\varphi/dt = -c_1\,\varphi$). The basic elements of an automatic controller are first, an element which measures the output of the system; second, a means for comparing that output with the desired one; and third, a means for feeding back this information into the input in such a way as to minimize the deviation of the output from the desired level. This means, in the case of directed movement, that the cell must have the ability to measure its orientation with respect to the applied polar guiding field. The created intracellular signal is such that the cell rotates to approach the desired orientation. The action of the automatic controller involved in directed movement can be investigated by changing the guiding field. The mean migration direction approaches the new direction by a single exponential function [34,41,42]. The characteristic time of this relaxation process is c_1^{-1} (in the absence of noise).

The second term $\Gamma_\varphi(t)$ on the right side of Eq. (3) characterizes stochastic processes in the cellular signal transduction-response system. The existence of these stochastic processes is evident if the migration behavior is regarded in the absence of a guiding field: a random walk is observed. The limitations of this crude approxi-

mation of the cellular machinery are discussed at the end of this article.

FOKKER-PLANCK EQUATION

In the case of deterministic differential equations [$\Gamma(t) = 0$], the behavior of a single cell or of an inert particle can be predicted. But in the case of a stochastic differential equation, only the probability for the behavior of a cell or of an inert particle can be given.

Our problem is to solve a stochastic differential equation like Eq. (1), (2), or (3). But *solving* a stochastic differential equation is not the same thing as solving any ordinary differential equation since the function $\mathbf{\Gamma}(t)$ has only statistically defined properties. Consequently, *solving* a Langevin equation has rather to be understood in the sense of specifying a probability density e.g., $W(v,t;v_0)$ or $W(\varphi,t;\varphi_0)$, which governs the probability of occurrence of the speed v or of the angle φ at time t.

To proceed further, one has to know some properties of the stochastic term, Γ(t). First, one assumes that its average should be zero,

$$\langle\Gamma(t)\rangle = 0, \tag{4}$$

because the average speed, for example, should be given by the Langevin equation without the stochastic term. If the stochastic processes are approximated by a white noise source, the autocorrelation function of $\Gamma(t)$ is then

$$\langle\Gamma(t)\Gamma(t')\rangle = q\,\delta(t-t'), \tag{5}$$

where q describes the strength of the white noise source. The white noise assumption in the case of directed movement will be discussed at the end of this article.

The equation of motion for the distribution function $W(v,t)$ is the Fokker-Planck equation which can be derived from a Langevin equation [like Eq. (1), (2), or (3)]. The general Fokker-Planck equation for one variable, e.g., v, has the form [31]

$$\frac{\partial W}{\partial t} = \left(-\frac{\partial}{\partial v}D^{(1)}(v) + \frac{\partial^2}{\partial v^2}D^{(2)}(v)\right)W(v,t). \tag{6}$$

The drift coefficient $D^{(1)}(v)$ is obtained from the deterministic part of the Langevin equation, e.g., from Eq. (2) one obtains $D^{(1)}(v) = \gamma_v(v_s - v)$. The coefficient $D^{(2)}(v)$ is obtained from the stochastic part of a Langevin equation. In the case of white noise one obtains $D^{(2)} = q/2$.

Stationary solution

For stationary solutions, the probability current $\frac{\partial W}{\partial t}(=0)$ in Eq. (6) must be constant. Thus one obtains a Gaussian distribution for the velocity

$$W(v) = W_0\, e^{-\frac{2}{q}(v-v_s)^2}. \tag{7}$$

W_0 is determined by normalization. Such a distribution was actually found for migrating granulocytes [14,33]. The stationary velocity distribution function for the Brownian motion process of inert particles described by the Langevin equation [Eq. (1)] leads immediately to the Maxwell distribution

$$W(v) = W_0\, e^{-\frac{mv^2}{2kT}}. \tag{8}$$

In Brownian motion the noise strength q is adjusted so that the average energy is given by the equipartition law of classical statistical mechanics (movement in two dimensions) [31],

$$q = \frac{2\gamma kT}{m}, \tag{9}$$

where kT is the thermal energy and m the mass of the inert particle.

The Fokker-Planck equation for the angle distribution function can be obtained from Eq. (3) as

$$\frac{\partial W}{\partial t} = c_1\frac{\partial}{\partial\varphi}[W(\varphi,t)\sin\varphi] + \frac{q}{2}\frac{\partial^2 W(\varphi,t)}{\partial\varphi^2}. \tag{10}$$

The stationary solution then reads

$$W(\varphi) = W_0\, e^{\frac{2c_1}{q}\cos\varphi}, \tag{11}$$

where W_0 is determined by normalization. This polar distribution induced by an electric guiding field was verified for migrating granulocytes [43,44], for migrating fibroblasts [35], for migrating neural crest cells [37], and for growing hyphae [45].

The polar order parameter as the average of $\cos\varphi$ can be used to quantify the directed movement. One obtains an analytic expression for the dose-response curve ($\langle\cos\varphi\rangle$ as a function of the guiding field c_1) (two dimensions)

$$\langle\cos\varphi\rangle = \frac{I_1(\frac{2c_1}{q})}{I_0(\frac{2c_1}{q})}, \tag{12}$$

where I_1 and I_0 are hyperbolic Bessel functions. This theoretical expression for the dose-response curve is very general since the polar guiding field is written in dimensionless units, $2c_1/q$. It is the ratio of the deterministic and the stochastic torque. Data are shown in Fig. 3 for migrating granulocytes [32,34], migrating somitic fibroblasts [36], and migrating spermatozoids [44]. In case of galvanotaxis the coefficient c_1 is proportional to the electric-field strength E [32,34],

$$c_1 = k_P\, E. \tag{13}$$

The coefficient k_P quantifies the automatic controller with respect to electric guiding fields. The actual fitting parameter is the galvanotactic coefficient, K_G, with $2c_1/q = K_G E$. The coefficient K_G can be determined either by the angle distribution function at different field strengths or by the galvanotactic dose-response curve.

The chemotaxis can be treated in the same way as galvanotaxis. The electric guiding field has to be replaced by the concentration gradient of the stimulating

molecules [c]. The torque should be proportional to grad ln [c], as actually found [43]. There is a problem, however, since the constant of proportionality is a function of the mean concentration [c], of the chemotactic molecule. The chemotactic sensitivity is maximal if the mean concentration of the chemotactic molecules is equal to the equilibrium binding constant K_R of the corresponding cellular membrane-bound receptor [38]. In the case of chemotaxis, the coefficient c_1 in Eq. (3) has to be exchanged by [34,43,47]

$$c_1 = K^0_{\mathrm{CT}} \frac{K_R[c]}{(c+K_R)^2} \frac{1}{[c]} \frac{d[c]}{dx}. \tag{14}$$

The experimentally determined value for $K^0_{\mathrm{CT}} (= \frac{2k^0_{\mathrm{CT}}}{q})$ is 9 mm [43] in the case of granulocytes. The theoretical predictions demonstrated for galvanotaxis hold true also for chemotaxis.

The dose-response curve thus holds true for different types of directed movement such as chemotaxis, galvanotaxis, etc., for different types of directed growth like chemotropism, galvanotropism, etc., as well as for different cell types (see Fig. 3). It holds true for granulocytes exposed to two different types of guiding fields (concentration gradient and electric field), but also for cells which have completely different migration mechanisms. Granulocytes, fibroblasts, and neural crest cells have an amoeboid movement where the cell shape is continously changing in time. These cells continously change their adherence to the substrate. Bracken spermatozoids of fern have a fixed shape and can swim in water. These cells are pushed by a moving flagellum. The dose-response curve holds true for this cell if it is forced to swim in a narrow gap and guided by an electric field or concentration gradient. The galvanotaxis coefficient K_G quantifying the cellular sensitivity to the electric guiding field is considerably different for the investigated cells: -4.5 mm/V for granulocytes, $+3.3$ mm/V for somitic fibroblasts, $+6.7$ mm/V for neural crest cells, and 42 mm/V for bracken spermatozoids. (The sign indicates in which direction the cell moves, $-$ to the anode and $+$ to the cathode.) Besides the directed movement a few experimental data points are shown for directed growth: *Fucus* eggs in a pH gradient and an electric field and the hyphae (roots) of *Neurospora crassa* in an electric field.

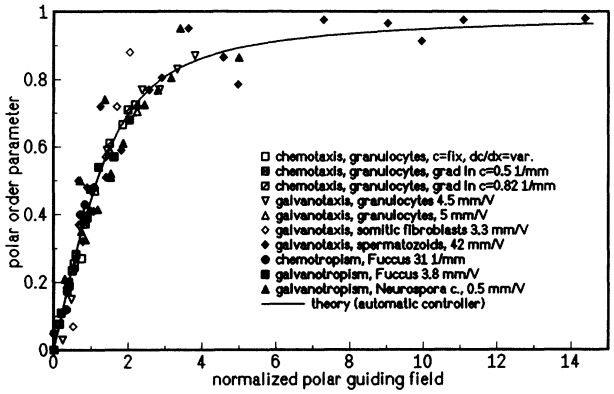

FIG. 3. Dose-response curve. The directed movement characterized by the polar order parameter is the cellular response induced by a polar guiding field which can be an electric field or a concentration gradient of chemotactically active molecules. The polar fields are given in dimensionless units, galvanotaxis $K_G E$ and chemotaxis $K_{\mathrm{CT}} \frac{dc}{c\,dx}$ [see Eq. (15)]. Chemotaxis of granulocytes $K^0_{\mathrm{CT}} = 9$ mm and $K_R = 6.6\mu M$ f-Met-Met-Met (data from Ref. [38]). Galvanotaxis of granulocytes $K_G = -4.5$ mm/V (data from Ref. [34]) and $K_G = -5$ mm/V (data from Ref. [32]). Galvanotaxis of somitic fibroblasts $K_G = 3.3$ mm/V (data from Ref. [36]). Galvanotaxis of bracken spermatazoids $K_G = 42$ mm/V (data from Ref. [46]). Chemotropism of *Fucus* eggs $K^{-1}_{\mathrm{CT}} = 3.2$ mm (data from Ref. [49]). Galvanotropism of *Pelvetia* eggs $K_G = -3.8$ mm/V (data from Ref. [50]). Galvanotropism of *Neurospora crassa* $K_G = 0.5$ mm/V (data from Ref. [51]).

Nonstationary solution

The machine coefficient q responsible for the random movement can be determined in different ways [14]. (1) The analysis of the time-dependent angle distribution as obtained from guiding-field jump experiments, or (2) the analysis of the angle autocorrelation function, or (3) the analysis of the mean-squared displacement.

Let us discuss the situation where the applied guiding field is constant in given time intervals and thus the coefficients of the Fokker-Planck equation [Eq. (10)] are constant. One can then make the separation ansatz

$$W(\varphi, t) = \Theta(\varphi) e^{-\lambda t}. \tag{15}$$

Inserting Eq. (15) into the Fokker-Planck equation leads to the following eigenvalue equation:

$$L_{\mathrm{FP}} \Theta(\varphi) = -\lambda \Theta(\varphi), \tag{16}$$

where L_{FP} is the Fokker-Planck operator

$$L_{\mathrm{FP}} = \frac{\partial}{\partial \varphi} \left(c_1 \sin\varphi + \frac{q}{2} \frac{\partial}{\partial \varphi} \right). \tag{17}$$

For nonvanishing guiding field ($c_1 \neq 0$) the operator L_{FP} is a non-Hermitian operator and therefore calculations become difficult [14]. The unknown function $\Theta(\varphi)$ in the separation ansatz Eq. (15) can be expressed by a Fourier series as the problem is periodic with 2π.

$$\Theta(\varphi) = \sum_{n=-\infty}^{\infty} c_n e^{in\varphi} \tag{18}$$

with $c_n = c^*_{-n}$ and $c_n = a_n - ib_n$.

The following equations (n between $+\infty$ and $-\infty$) are obtained by inserting Eq. (18) in Eq. (16):

$$\frac{n}{2} E k_P c_{n-1} + \left(\lambda - n^2 \frac{q}{2} \right) c_n - \frac{n}{2} k_P E c_{n+1} = 0. \tag{19}$$

From this equation, the eigenvalues λ and the Fourier coefficients c_n are calculated. It is worth mentioning that the coefficients can be chosen purely imaginary or purely

real. In the first case, one obtains an antisymmetric solution, in the last case a symmetric solution of Eq. (19).

For vanishing guiding field E, the system reduces to

$$\left(\lambda - n^2 \frac{q}{2}\right) c_n = 0. \tag{20}$$

The eigenvalues λ_μ are

$$\lambda_\mu = \mu^2 \frac{q}{2}. \tag{21}$$

The μth eigenfunction reads

$$\Theta_\mu(\varphi) = 2a_\mu^\mu \cos \mu\varphi + 2b_\mu^\mu \sin \mu\varphi. \tag{22}$$

For nonvanishing guiding field ($c_1 \neq 0$), the eigenvalues $\lambda(c_1)$ were obtained from the tridiagonal system [Eq. (19)] by using the method of continued fractions as described by Risken [31]. The calculations of the continued fractions and the determination of the roots were made numerically. The first four nonvanishing eigenvalues λ as a function of the normalized guiding-field strength ($\frac{2c_1}{q} = \frac{2k_P E}{q} = K_G E$) are shown in Fig. 4. For low normalized guiding-field strength ($K_G E \ll 1$), the eigenvalues are approximately constant, as expected. At large guiding-field strengths, the eigenvalues increase with increasing field strength. The latter result is expected if the stochastic term in Eq. (10) is neglected,

$$\lambda_n(E) = n c_1 = n k_P E. \tag{23}$$

The stochastic differential equation [Eq. (10)] can be solved analytically [48] if the stochastic term is regarded as a perturbation,

$$\lambda_n(E) = n c_1 - \frac{q}{4} n^2 = n\, k_P\, E - \frac{q}{4} n^2. \tag{24}$$

The straight line is shifted out of the origin and holds true for large polar guiding-field strengths. The stochastic differential equation [Eq. (10)] can also be solved analytically [48] if the deterministic term is regarded as a perturbation,

$$\frac{\lambda_n(E)}{\lambda_1(0)} = n^2 + \frac{1}{2} \frac{n^2}{4n^2 - 1} \left(\frac{2c_1}{q}\right)^2 + \cdots = n^2 + \frac{1}{2} \frac{n^2}{4n^2 - 1} (K_G E)^2 + \cdots. \tag{25}$$

The parabola near the origin holds true for small polar guiding fields. The exact solution is approximated quite well by the straight line and the parabola as shown in Fig. 4.

The normalized eigenvalues $\frac{\lambda_n(E)}{\lambda_1(0)}$ with $\lambda_1(0) = \frac{q}{2}$ and the normalized guiding field strength $\frac{2c_1}{q} = K_G E$ are dimensionless quantities. A plot of the normalized eigenvalues versus normalized field strength gives a universal curve which should hold true for different cell types (Fig. 5) if the cellular machinery is a proportional controller.

Knowing the eigenvalues, it is possible to calculate the corresponding eigenfunctions $\Theta(\varphi)$ from Eq. (16), which are degenerate: for each eigenvalue we find two eigenfunctions. The symmetric one is obtained if c_n is real and the antisymmetric if c_n is imaginary. Because the eigenfunctions are not orthonormalized, one has to transform the operator $L_{\rm FP}$ into a Hermitian one. One proceeds as shown in Ref. [31]. A new operator L is introduced

$$L = e^{+\frac{\Phi}{2}} L_{\rm FP}\, e^{-\frac{\Phi}{2}}, \tag{26}$$

with $\Phi = \frac{2c_1}{q} \cos\varphi = K_G E \cos\varphi$. L is a Hermitian operator which has the same eigenvalues λ as the operator $L_{\rm FP}$. The eigenfunctions of L are given by

$$\theta_\mu^i(\varphi) = e^{\frac{\Phi}{2}}\, \Theta_\mu^i(\varphi). \tag{27}$$

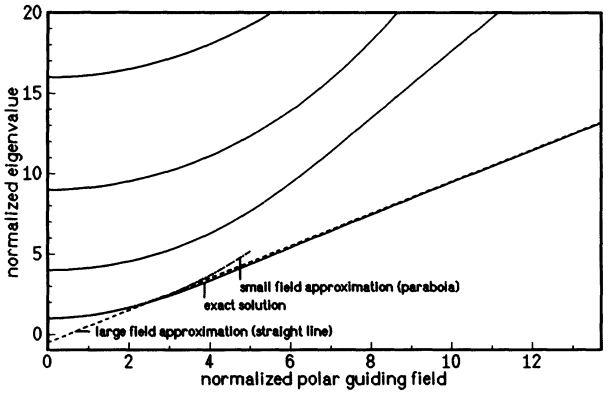

FIG. 4. The calculated first four eigenvalues λ as a function of normalized polar guiding field $K_G E$ are shown for human granulocytes [$K_G = 4.5$ mm/V and $\lambda_1(0)^{-1} = 58$ s]. The dashed straight line is the high field approximation. The dash-dotted parabolic line is the small field approximation.

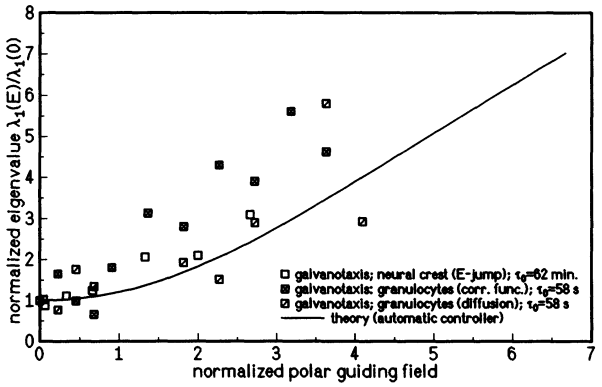

FIG. 5. The normalized first eigenvalue as a function of normalized guiding-field strength $K_G E$. The values $K_G = 4.5$ mm/V and $\lambda_1(0)^{-1} = \tau_0 = 58$ s for migrating granulocytes were taken from the data from Refs. [34,41]. The angle autocorrelation function (data from Ref. [34]) and the mean-squared displacement (original trajectory data of Ref. [34]) were used to determine the first eigenvalue $\lambda_1(E)$. E-jump experiments (data from Ref. [42]) were used to determine the first eigenvalues of neural crest cells [$K_G = 6.7$ mm/V and $\lambda_1(0)^{-1} = \tau_0 = 62$ min].

Now Eq. (10) can be solved, resulting in time-dependent distribution functions. The distribution function is then given by the expression

$$W(\varphi,t) = W_{\rm st}(\varphi) + \sum_{\mu=1}^{\infty} e^{-\lambda_\mu t}[d^s_\mu \Theta^s_\mu(\varphi) + d^a_\mu \Theta^a_\mu(\varphi)]. \tag{28}$$

The constants d^i_μ follow from the initial distribution. $W_{\rm st}(\varphi)$ is the stationary angle distribution function.

Eigenvalues

One way to determine the eigenvalues is to perform guiding-field jump studies. For example, the electric field is switched on at $t = 0$. Thus for $t < 0$, no directed movement is expected and the angular distribution function is a horizontal line as expected for isotropic random movement. For $t > 0$, the applied electric field induces a directed movement. Instead of investigating the entiere distribution function, only the polar order parameter is taken into consideration,

$$\langle \cos\varphi(t)\rangle = \langle \cos\varphi\rangle_{\rm st} + 2\pi \sum_{\mu=0}^{\infty} e^{-\lambda_\mu t} d^s_\mu c^\mu_1. \tag{29}$$

Electric-field jump experiments were performed for migrating granulocytes and migrating neural crest cells. The polar order parameter as a function of time can be approximated by a single exponential function [34]. Thus the first eigenvalue is obtained as a function of the applied field strength. Unfortunately, only experiments using two different field strengths were performed for granulocytes. More experiments were performed for neural crest cells [42]. The results are shown in Fig. 5.

The eigenvalues can also be determined from the angle autocorrelation function. One has to calculate the expression

$$\begin{aligned} g^s_\varphi &= \langle \cos\varphi(t)\cos\varphi(t')\rangle \\ &= \int_0^{2\pi} d\varphi \cos\varphi \int_0^{2\pi} d\varphi' \cos\varphi'\, P(\varphi,t|\varphi',t')\, W_{\rm st}(\varphi') \\ &= \frac{N\sum_{\mu=1}(2\pi c^\mu_1)^2 e^{-\lambda_\mu|t-t'|} + (2\pi c^0_1)^2}{N\sum_{\mu=1}(2\pi c^\mu_1)^2 + (2\pi c^0_1)^2}, \end{aligned} \tag{30}$$

where N is a calibration coefficient obtained from the stationary angle distribution function $[\int_0^{2\pi} W(\varphi)d\varphi = 1]$ and $P(\varphi,t|\varphi',t')$ is the transition probability. The saturation value of the angle autocorrelation function is given by the steady state polar order parameter $\langle\cos\varphi\rangle$, since $\langle\cos\varphi\rangle_{\rm st} = 2\pi c^0_1$. A similar angle autocorrelation function can be calculated with respect to $\sin\varphi$,

$$\begin{aligned} g^a_\varphi &= \langle \sin\varphi(t)\sin\varphi(t')\rangle \\ &= \int_0^{2\pi} d\varphi \sin\varphi \int_0^{2\pi} d\varphi' \sin\varphi'\, P(\varphi,t|\varphi',t')\, W_{\rm st}(\varphi') \\ &= \frac{\sum_{\mu=1}(2\pi b^\mu_1)^2 e^{-\lambda_\mu|t-t'|}}{\sum_{\mu=1}(2\pi c^\mu_1)^2}. \end{aligned} \tag{31}$$

Note that $\langle\sin\varphi\rangle_{\rm st} = 2\pi b^0_1 = 0$. The calculated stationary angle autocorrelation functions $\langle\cos\varphi(t)\cos\varphi(t')\rangle$ and $\langle\sin\varphi(t)\sin\varphi(t')\rangle$ are shown in Fig. 6. The measured stationary angle autocorrelation function $\langle\cos\varphi(t)\cos\varphi(t')\rangle$ is a single exponential decay function for migrating granulocytes as predicted [34]. The normalized first eigenvalues $\frac{\lambda_1(E)}{\lambda_1(0)}$ as a function of the normalized electric field $K_G E$ are shown in Fig. 5. (The eigenvalues for large fields are not very accurate due to experimental limitations.)

The eigenvalues can also be determined from the mean-squared displacement as a function of time. Here one is interested in the mean-squared displacement $\langle y(t)^2\rangle$ perpendicular to the electric field. The mean-squared displacement is directly related to the stationary angle autocorrelation function [Eq. (31)].

The displacement is given by

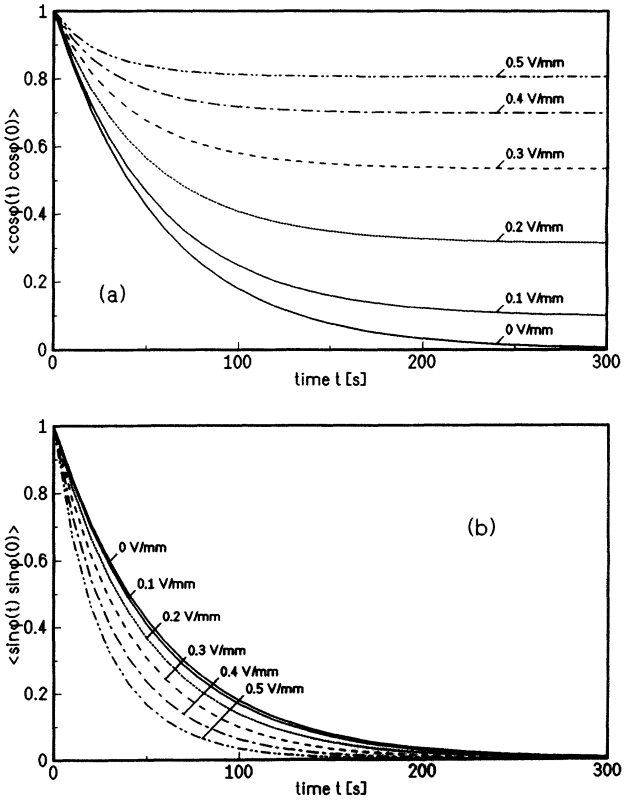

FIG. 6. Angle autocorrelation functions as a function of the guiding field are shown. (a) $\langle\cos\varphi(t)\cos\varphi(0)\rangle$, calculated from the symmetric function and (b) $\langle\sin\varphi(t)\sin\varphi(0)\rangle$, calculated from the antisymmetric function.

$$y = \int_0^t v(t') \sin\varphi(t') dt'. \tag{32}$$

The mean-squared displacement $\langle y(t)^2 \rangle$ then reads

$$\langle y(t)^2 \rangle = \left\langle \left[\int_0^t v(t') \sin\varphi(t') dt' \right]^2 \right\rangle. \tag{33}$$

Taking advantage of the fact that $v(t)$ and $\varphi(t)$ are statistically independent from each other one derives [14]

$$\begin{aligned} \langle y(t)^2 \rangle &= 2 \int_0^t \int_0^{t_1} \langle v(t_1) v(t_2) \rangle \langle \sin\varphi(t_1) \sin\varphi(t_2) \rangle dt_2 dt_1 \\ &= 2\langle v^2 \rangle \int_0^t \int_0^{t_1} \langle \sin\varphi(t_1) \sin\varphi(t_2) \rangle dt_2 dt_1. \end{aligned} \tag{34}$$

After performing the integration, one obtains

$$\langle y(t)^2 \rangle = 8\pi^2 N \langle v^2 \rangle \sum_\mu \frac{1}{\lambda_\mu} \left(t - \frac{1}{\lambda_\mu} (1 - e^{-\lambda_\mu t}) \right) (b_1^\mu)^2. \tag{35}$$

For large times, one obtains the diffusion coefficient D_y as

$$D_y = 4\pi^2 N \langle v^2 \rangle \sum \frac{(b_1^\mu)^2}{\lambda_\mu}. \tag{36}$$

In the case of no guiding field, one obtains a random walk with $b_1^\mu \neq 0$ for $\mu \geq 1$. In the case of a polar guiding field, only the first eigenvalue was used to fit the experimental data ($\langle y^2 \rangle$ vs time). Equation (35) is fitted to the previously published experimental data [34] where the first eigenvalue λ_1 and the diffusion coefficient D_y are the fitting parameters. The eigenvalues are shown in Fig. 5. The characteristic time τ ($= 1/\lambda_1$) and the ratio of the diffusion coefficient D_y and the mean-squared speed $\langle v^2 \rangle$ are shown in Fig. 7. The experimentally determined values are in accordance with the predicted normalized curve which is based on the galvanotaxis coefficient $K_G = \frac{2k_P}{q}$ obtained from the measured dose-response curve, and on the measured first eigenvalue $\lambda_1(0) = \frac{q}{2}$, when no field was applied.

The normalized dose-dependent eigenvalue curve should hold true for different types of directed movement such as chemotaxis and galvanotaxis, etc. The predicted curve is compared with experimental data obtained from granulocytes and neural crest cells exposed to electric guiding fields. The characteristic time $\tau(0)$ characterizing the random walk is considerably different for these two cell types: 58 s for granulocytes and 60 min for neural crest cells.

Finally we will ask which temperature corresponds to the random movement of cells. This comparison can be made by means of the diffusion coefficient. The diffusion coefficient D is the ratio of the mean-squared speed $\langle v_0^2 \rangle$ and the coefficient q_φ which quantifies the stochastic processes in the automatic controller,

$$D = \frac{1}{2} \frac{\langle v_0^2 \rangle}{q_\varphi}. \tag{37}$$

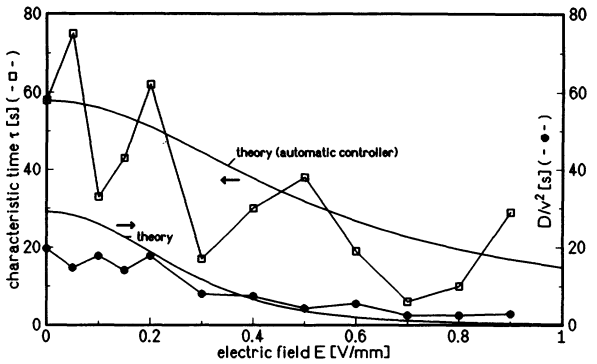

FIG. 7. Diffusion coefficient D_y divided by the mean-squared speed $\langle v^2 \rangle$ and the characteristic time τ as a function of guiding-field strength E are shown for migrating granulocytes. The characteristic time $\tau(E)$ and the diffusion coefficient $D_y(E)$ as a function of the applied polar guiding field E are calculated [$K_G = -4.5$ mm/V and $\lambda_1(0)^{-1} = 58$ s] and shown as solid lines. The dots originate from trajectories of migrating cells [original data of Ref. [34]]. The random walk perpendicular to the applied guiding field was evaluated. The characteristic time τ and the diffusion coefficient D_y were obtained by fitting Eq. (35) to the data.

The Einstein relation applied to an inert particle connects the diffusion coefficient D the mobility R and the thermal energy kT,

$$DR = kT. \tag{38}$$

The mobility of a spherical particle with radius r in a viscous medium with a viscosity η is given by Stokes,

$$R = 6\pi\eta r. \tag{39}$$

Thus the random movement of a migrating cell ($D = 200\ \mu m^2/min$) corresponds to a very high temperature, 4.5×10^4 K ($r = 10\ \mu$m, $\eta = 0.01$ P).

LIMITATIONS OF THE MODEL

The migration or growth of cells is quite well approximated by the simple stochastic differential equation [Eq. (3)] which is derived for an automatic proportional controller (with noise). The $\sin\varphi$ dependence of the deterministic term is verified by the steady state angle distribution function [44]. The linear response of the cell with respect to a polar guiding field is verified by the dose-response curve (Fig. 3). The white noise assumption is in accordance with random walk behavior and with the field-dependent first eigenvalue (Fig. 5). The machine coefficients k_P and q for the galvanotactic response can be determined, e.g., from the dose-response curve and the mean-squared displacement in the absence of a guiding field. Thus the cellular behavior can be predicted in different situation.

First a guiding-field jump experiment is performed as described above. The polar order parameter is measured

and compared with the prediction. The following absolute values of the characteristic times were obtained. $\tau_{\text{expt}} = 32$ s and $\tau_{\text{theor}} = 15$ s for granulocytes exposed to +1 V/mm and −1 V/mm [34]; $\tau_{\text{expt}} = 42$ s and $\tau_{\text{theor}} = 20$ s for granulocytes exposed to +0.8 V/mm and −0.8 V/mm [41]; $\tau_{\text{expt}} = 200$ s and $\tau_{\text{theor}} = 90$ s for granulocytes exposed to no guiding field and then to pulsed electric field ($E_1 = 0.8$ V/mm, $t_1 = 1$ s, $E_2 = 0$ V/mm, $t_2 = 7$ s) [41]. These systematic deviations show us that the model of the automatic controller has to be improved.

These systematic deviations are very likely produced by the crude approximation of the cellular signal transduction-response system by the Langevin equation with a white noise source. The transfer function of the cellular signal transduction-response system is certainly not frequency independent as assumed in the case of the white noise source. The self-ignition model as described in the Introduction is a possible mechanism involved in directed and nondirected movement. Thus one expects correlations in the stochastic term $\Gamma(t)$, since the molecular events of the cellular signal chain are expected to be correlated. The frequency-dependent cellular signal transfer function is determined in part by using pulsed fields. From preliminary experiments we know that a characteristic time of 8 s plays an important role in the cellular signal chain of granulocytes. (i) The cellular response is enhanced by pulsed electric fields having a characteristic time of 8 and 16 s [41]. (ii) There exists a delay time of 8 s between the time of application of the guiding field and the time of the first cellular response [34,41]. These two experimental facts are demonstrated in Fig. 8. For $t < 0$ no guiding field was applied, the cell showed a random walk, and the polar order parameter was zero. At t=0 a pulsed guiding field is switched on ($E_1 = +0.8$ V/mm, $t_1 = 16$ s, $E_2 = -0.8$ V/mm, $t_2 = 16$ s). The delay time as well as the enhanced cellular response expected from the self-ignition model are demonstrated.

There is a further remarkable deviation between the simple Langevin equation and the cellular response which can be seen by averaging over one period. The results are shown in Fig. 8. The predicted, like the actual measured averaged response, showed a peak after switching on the guiding field. For larger times the averaged response should approach zero. But actually one found a broad peak opposite to the first one.

The cellular signal transduction-response system of a migrating cell was approximated in part by a white noise. This assumption was introduced due to its simple mathematical treatment but we were aware that a white noise is not a good description for a machine having typical rhythms. Thus we were surprised that this crude assumption yields such good results, like the prediction of the steady state behavior. The white noise assumption failed as soon as we tried to predict the temporal behavior. To proceed further, simplified rate equations which are closely related to the cellular biochemical events will be discussed.

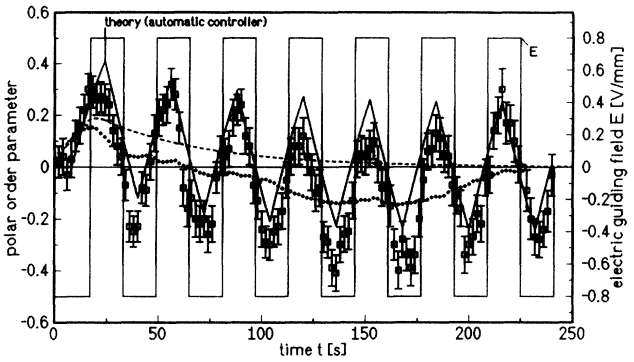

FIG. 8. Polar order parameter as a function of pulsed electric guiding field ($E_1 = +0.8$ V/mm, $t_1 = 16$ s, $E_2 = -0.8$ V/mm, $t_2 = 16$ s). For $t < 0$ no guiding field was applied. At $t = 0$ the pulsed guiding field was switched on. The dots with the error bars (standard deviation of the mean) are the experimental results. The zigzag line is a theoretical prediction [$-K_G = -4.5$ mm/V, $2/q = 58$ s white noise assumption]. The predicted curve is altered in the following ways: (i) The calculated polar order parameter is multiplied by 1.6 (enhanced cellular sensitivity) and (ii) the time axis is shifted by 8 s (cellular lag time). The modified predicted curve fits the experimental dots quite well. The dotted line is obtained by averaging over 32 s of the experimental results. The dashed line is the corresponding modified theoretical prediction.

ACKNOWLEDGMENTS

We are grateful to Professor Marcel Bessis and Dr. Anne de Boisfleury-Chevance for their support and encouragement. This work was supported in part by "Fond der chemischen Industrie," "Deutsche Forschungsgemeinschaft," "Deutscher Akademischer Austauschdienst" and "Fondation de France."

[1] *Lecture Notes in Biomathematics. Biological Motion*, edited by W. Alt and G. Hoffmann (Springer-Verlag, Heidelberg, 1990).

[2] P.C. Wilkinson, *Chemotaxis and Inflammation* (Churchill, London, 1974).

[3] J.P. Trinkaus, *Cells into Organs* (Prentice-Hall Inc., Englewood Cliffs, NJ, 1984).

[4] E.L. Becker, Y. Kanaho, and J.C. Kermode, Biomed. Pharmacother. **41**, 289 (1987).

[5] D.R. Williams and P.G. deGennes, Europhys. Lett. **24**, 311 (1993).

[6] G. F. Oster and A. S. Perelson, J. Cell Sci. Suppl. **8**, 35 (1987).

[7] H. Gruler, in *Chaos and Complexity*, edited by J.T. Thanh Van (Editions Frontières, Gif sur Yvette, in press).

[8] H.-U. Keller and M. Bessis. Nouv. Rev. Fr. Hematol. **15**, 439 (1975).

[9] H. Gruler and A. de Boisfleury-Chevance, Z. Naturforsch. Teil C **42**, 1126 (1987).
[10] S. Malavista, Ann. N. Y. Acad. Sci. **466**, 858 (1988).
[11] H. Gruler, in *Lecture Notes in Biomathematics. Biological Motion* (Ref. [1]).
[12] H. Gruler and K. Franke, Z. Naturforsch. Teil C **45**, 1241 (1990).
[13] H. Gruler, in *Biologically Inspired Physics*, edited by L. Peliti (Plenum Press, New York, 1991).
[14] M. Schienbein and H. Gruler, Bull. Math. Biol. **55**, 585 (1993).
[15] R. Brown, Pogg. Ann. **14**, 294 (1828).
[16] K. Pearson, Nature **77**, 294 (1905).
[17] Lord Rayleigh, Philos. Mag. **10**, 73 (1880); **47**, 246 (1889).
[18] R. Fürth, *A. Einstein, Investigations on the Theory of the Brownian Movement* (Dover, New York, 1956).
[19] M. v. Smoluchowski, Bull. Acad. Cracovie, **1906**, 206 (1906).
[20] R. Fürth, *Schwankungserscheinungen in der Physik* (Vieweg, Braunschweig, 1920).
[21] P. Langevin, C. R. Acad. Sci. **146**, 530 (1908).
[22] N. Wax, *Noise and Stochastic Processes* (Dover, New York, 1954).
[23] W. Schottky, Ann. Phys. (Leipzig) **57**, 541 (1918).
[24] W. Schottky, Ann. Phys. (Leipzig) **68**, 157 (1922).
[25] H. Nyquist, Phys. Rev. **32**, 110 (1928).
[26] M. Lax, Rev. Mod. Phys. **32**, 25 (1960).
[27] H. Haken, *Synergetics* (Springer, Berlin, 1983).
[28] H.A. Kramers, Physica **7**, 284 (1940).
[29] *Noise in Nonlinear Dynamical Systems*, edited by F. Moss and P.V.E. McClintock (Cambridge University Press, Cambridge, England, 1989).
[30] N. Wiener, *Cybernetics: Or Control and Communication in Animal and the Machine* (MIT Press, Cambridge, 1961).
[31] H. Risken, *Fokker-Planck Equation* (Springer-Verlag, Heidelberg, 1984).
[32] B. Rapp, A. de Boisfleury-Chevance, and H. Gruler, Eur. Biophys. J. **16**, 313 (1988).
[33] H. Gruler, Blood Cells **10**, 107 (1984).
[34] K. Franke and H. Gruler, Eur. Biophys. J. **18**, 335 (1990).
[35] H. Gruler and R. Nuccitelli, in *Ionic Currents in Development*, edited by R. Nuccitelli (Liss Corp., New York, 1986).
[36] C.A. Erickson and R. Nuccitelli, J. Cell Biol. **98**, 296 (1984).
[37] H. Gruler and R. Nuccitelli, Cell Motil. Cytoskeleton **19**, 121 (1991).
[38] S.H. Zigmond, J. Cell. Biol. **75**, 606 (1977).
[39] L.E. Becker, H.J. Showell, P.H. Naccache, and R. Sha'afi, in *Leukocyte Chemotaxis Methods, Physiology, and Clinical Implications*, edited by J.I. Gallin and P.G. Quie (Raven Press, New York, 1978), pp. 113.
[40] J. Maher, J.V. Martell, B.A. Brantley, E.B. Cox, J.E. Niedel, and W.F. Ross, Blood **64**, 221 (1984).
[41] K. Franke and H. Gruler, Z. Naturforsch. Teil C **49**, July (1994).
[42] H. Gruler and R. Nuccitelli (unpublished).
[43] H. Gruler, Z. Naturforsch. Teil C **43**, 754 (1988).
[44] H. Gruler, in *The Cellular Biochemistry and Physiology of Neutrophil*, edited by M.B. Hallett (Chemical Rubber, Boca Raton, 1989).
[45] H. Gruler and N.A.R. Gow, Z. Naturforsch. Teil C **45**, 306 (1990).
[46] J.C. Brokaw. J. Exp. Biol. **35**, 197 (1958).
[47] R.T. Tranquillo, S.H. Zigmond, and D.A. Lauffenburger, Cell Motil. Cytoskeleton **11**, 1 (1988).
[48] H.D. Vollmer and H. Risken, Physica **110A**, 106 (1982).
[49] F. Bentrup, T. Sandau, and L. Jaffe, Protoplasma **64**, 254 (1967).
[50] H.P. Peng and L.F. Jaffe, Dev. Biol. **53**, 277 (1976).
[51] A.M. McGillivray and N.A.R. Gow, J. Gen. Microbiol. **132**, 2515 (1986).
[52] R.T. Tranquillo and D.A. Lauffenburger, J. Math. Biol. **25**, 229 (1987).

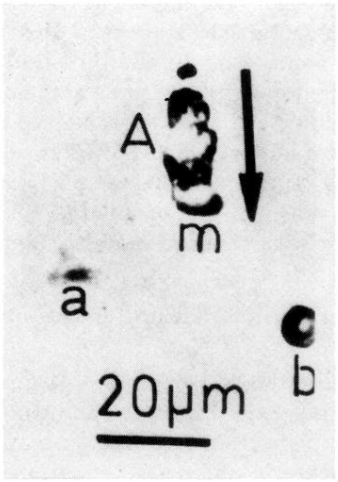

FIG. 1. Micrograph (phase contrast) of different blood cells in a sandwich cell [glass slide, aqueous solution (blood plasma, $d \approx 20\,\mu$m) coverslip]. (i) Human granulocyte (A) [leading front (m) and direction of migration (arrow)], (ii) platelet (a), and (iii) erythrocyte (b).